Progress In Electromagnetics Research Letters, Vol. 11, 173–181, 2009

MEASURE THE COMPLEX PERMEABILITY OF FERROMAGNETIC THIN FILMS: COMPARISON SHORTED MICROSTRIP METHOD WITH MICROSTRIP TRANSMISSION METHOD

Y. Wu, Z. Tang, Y. Xu, and B. Zhang

School of Electronic Engineering
University of Electronic Science and Technology of China
Chengdu 611731, China

Abstract—In this paper, two broadband measurement methods, shorted microstrip method and microstrip trnasmission method, are discussed, and the complex permeability of ferromagnetic thin films is measured from 100 MHz to 18 GHz. The S-parameters of the two measurement fixtures are measured by vector network analyzer (VNA). The perturbations of the thin film loaded in the measurement fixture are analyzed; the discontinuity between coaxial and microstrip is considered; the effective permeability is deduced from measured S-parameters; the permeability of ferromagnetic thin films is extracted from effective permeability by using conformal mapping. The results show that the experimental results agree with the theoretical ones closely, and higher measurement sensitivity and accuracy are achieved by using shorted microstrip method.

1. INTRODUCTION

A conventional technique for measuring microwave permittivity and permeability is filling a section of a standard closed transmission line, such as a waveguide or coaxial, with a large sample. However, this technique is ill suited for conductive materials, particularly when the sample under study is a low-resistive film [1]. For metal films deposited on a flexible polymer substrate, coaxial line perturbation method has good performance [2]. Whereas for the magnetic thin films deposited on rigid substrate, the planar transmission-line (i.e., microstrip [3–5]) methods are more suitable. The reason is that the

Corresponding author: Y. Wu (yunqiu_wu@hotmail.com).

thin film materials can be easily loaded in the measurement fixture. The shorted microstrip method (SMM) and microstrip transmission method (MTM) are two kinds of planar transmission-line methods. The SMM is a reflection technique adapted to a shorted or open microstrip, by measuring the reflection coefficients before and after loading the thin film in the fixture; the permeability of the thin film can be determined. And the MTM is a reflection-transmission technique adapted to a two-port microstrip transmission line [6]; the permeability of thin film can be obtained by analyzing the full S-parameters of the two ports.

In this paper, the complex permeability of ferromagnetic thin film is measured up to 18 GHz. Both of the SMM and MTM are discussed. The relations between network parameters and material permeability are analyzed, and the perturbations of the thin film loaded in the measurement fixture are investigated. The experimental results show that the complex permeability measured by SMM and MTM agrees with the theoretical results quite well, and the SMM can achieve a better performance in measurement sensitivity and accuracy compared with the MTM.

2. SHORTED MICROSTRIP METHOD

The measurement fixture of SMM is shown in Figure 1. The N-type coaxial connector is used to connect the fixture to the coaxial test port of vector network analyzer (VNA); the upper strip is made of copper; the ground plane and shorted plane are made of aluminum. In order to load samples in the fixture, the space between the upper strip and ground plane is left empty. When the sample is loaded in the fixture, the multilayer microstrip is constructed. To ensure the characteristic impedance of the microstrip close to 50 Ω, the width of the upper strip

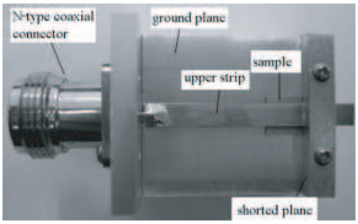

Figure 1. Measurement fixture of SMM.

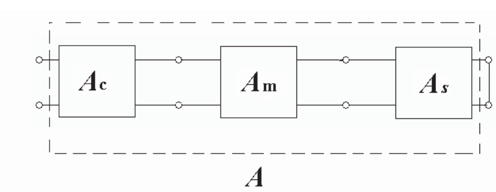

Figure 2. The schematic diagram of the shorted microstrip cascade network.

(w) is chosen as 4.15 mm, and the distance between the upper strip and ground plane (h) is chosen as 1 mm.

As shown in Figure 1, the fixture is cascaded from three transmission-line networks, which are coaxial line, microstrip line and multilayer microstrip line. The schematic diagram of the cascaded network is shown in Figure 2. A_c, A_m, and A_s are the ABCD matrix of coaxial line, microstrip line and multilayer microstrip line, respectively. After loading the substrate of the thin film in the fixture, the cascaded ABCD matrix can be expressed as

$$A_1 = \begin{bmatrix} \cosh(\gamma_1 l_1) & \sinh(\gamma_1 l_1) \\ \sinh(\gamma_1 l_1) & \cosh(\gamma_1 l_1) \end{bmatrix} \cdot \begin{bmatrix} \cosh(\gamma_0 l_2) & \frac{Z_c}{Z_0}\sinh(\gamma_0 l_2) \\ \frac{Z_0}{Z_c}\sinh(\gamma_0 l_2) & \cosh(\gamma_0 l_2) \end{bmatrix}$$
$$\cdot \begin{bmatrix} \cosh(\gamma_0 \sqrt{\varepsilon_{eff}}\, l_s) & \frac{Z_c}{Z_0\sqrt{\varepsilon_{eff}}}\sinh(\gamma_0 \sqrt{\varepsilon_{eff}}\, l_s) \\ \frac{Z_0\sqrt{\varepsilon_{eff}}}{Z_c}\sinh(\gamma_0 \sqrt{\varepsilon_{eff}}\, l_s) & \cosh(\gamma_0 \sqrt{\varepsilon_{eff}}\, l_s) \end{bmatrix} = \begin{bmatrix} a_1 & b_1 \\ c_1 & d_1 \end{bmatrix} \quad (1)$$

$$S_{11}^{sub} = \frac{b_1/d_1 - 1}{b_1/d_1 + 1} \quad (2)$$

where γ_1 and γ_0 are the transmission constant of coaxial and microstrip, respectively; Z_0 and Z_c are the characteristic impedance of coaxial and microstrip, respectively; (Z_0 is equal to $50\,\Omega$ here); l_1, l_2 and l_s are the length of coaxial, microstrip and multilayer microstrip, respectively; S_{11}^{sub} is the reflection coefficient with the substrate loaded in the fixture measured by VNA; ε_{eff} is the effective permittivity of the multilayer microstrip, which can be expressed as [7]

$$\varepsilon_{eff} = 1 - \sum_{i=1}^{3} q_i + \frac{\left(\sum_{i=1}^{3} q_i\right)^2}{\sum_{i=1}^{3} \frac{q_i}{\varepsilon_{ri}}} \quad (3)$$

where ε_{r1}, ε_{r2}, and ε_{r3} are the permittivity of the film, substrate and air, respectively; q_1, q_2 and q_3 are the corresponding filling factors and can be calculated from the equations list in appendix. When only the substrate is loaded in the fixture, q_1 is equal to zero.

Then the thin film deposited on the substrate is loaded in the fixture. Both the effective permittivity and effective permeability of the transmission line are changed. At the region where the thin film is inserted, as the electric field is perpendicular to the thin film, and the thickness of the thin film is very small, the change of the effective permittivity of the transmission line due to the insertion of the thin film is assumed to be negligible [6]. So the cascaded ABCD matrix can be expressed as

$$A_2 = \begin{bmatrix} \cosh(\gamma_1 l_1) & \sinh(\gamma_1 l_1) \\ \sinh(\gamma_1 l_1) & \cosh(\gamma_1 l_1) \end{bmatrix} \cdot \begin{bmatrix} \cosh(\gamma_0 l_2) & \frac{Z_c}{Z_0}\sinh(\gamma_0 l_2) \\ \frac{Z_0}{Z_c}\sinh(\gamma_0 l_2) & \cosh(\gamma_0 l_2) \end{bmatrix}$$

$$\cdot \begin{bmatrix} \cosh(\gamma_0\sqrt{\varepsilon_{eff}\mu_{eff}}l_s) & \frac{Z_c\sqrt{\mu_{eff}}}{Z_0\sqrt{\varepsilon_{eff}}}\sinh(\gamma_0\sqrt{\varepsilon_{eff}\mu_{eff}}l_s) \\ \frac{Z_0\sqrt{\varepsilon_{eff}}}{Z_c\sqrt{\mu_{eff}}}\sinh(\gamma_0\sqrt{\varepsilon_{eff}\mu_{eff}}l_s) & \cosh(\gamma_0\sqrt{\varepsilon_{eff}\mu_{eff}}l_s) \end{bmatrix}$$

$$= \begin{bmatrix} a_2 & b_2 \\ c_2 & d_2 \end{bmatrix} \tag{4}$$

$$S_{11}^{film} = \frac{b_2/d_2 - 1}{b_2/d_2 + 1} \tag{5}$$

where μ_{eff} is the effective permeability of the multilayer microstrip; S_{11}^{film} is the reflection coefficient with the film loaded in the fixture and measured by VNA. Solving Equations (1) $\sim$ (5), the effective permeability can be determined. And the perturbation of the thin film (ΔS_{11}) can be expressed as

$$\Delta S_{11} = \frac{S_{11}^{film}}{S_{11}^{sub}} \tag{6}$$

On the other hand, μ_{eff} can be deduced from Equation (3) by using duality principle [8]

$$\frac{1}{\mu_{eff}} = 1 - \sum_{i=1}^{3} q_i + \frac{\left(\sum_{i=1}^{3} q_i\right)^2}{\left(\sum_{i=1}^{3} q_i \mu_{ri}\right)} \tag{7}$$

where μ_{r1}, μ_{r2} and μ_{r3} are the permeability of thin film, substrate and air, respectively. The permeability of substrate and air are equal to 1. Then solving Equation (7), the permeability of thin film can be obtained as

$$\mu_r = \left(\frac{\left(\sum_{i=1}^{3} q_i\right)^2}{1/\mu_{eff} - 1 + \sum_{i=1}^{3} q_i} - q_2 - q_3 \right) / q_1 \tag{8}$$

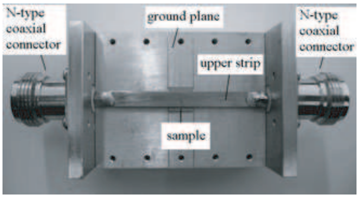

Figure 3. Measurement fixture of MTM.

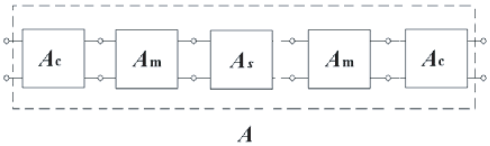

Figure 4. The schematic diagram of the microstrip transmission cascade network.

3. MICROSTRIP TRANSMISSION METHOD

The measurement fixture of MTM is shown in Figure 3. It is a symmetrical two ports configuration. As described in Section 3, to ensure that the characteristic impedance of the microstrip is close 50 Ω, the width of the upper strip (w) is chosen as 4.15 mm; the distance between the upper strip and ground plane (h) is also chosen as 1 mm.

The schematic diagram of the cascaded network is shown in Figure 4. The cascaded ABCD matrix after loading the substrate in the fixture can be expressed as

$$\begin{aligned} A_1 &= \begin{bmatrix} \cosh(\gamma_1 l_1) & \sinh(\gamma_1 l_1) \\ \sinh(\gamma_1 l_1) & \cosh(\gamma_1 l_1) \end{bmatrix} \cdot \begin{bmatrix} \cosh(\gamma_0 l_2) & \frac{Z_c}{Z_0}\sinh(\gamma_0 l_2) \\ \frac{Z_0}{Z_c}\sinh(\gamma_0 l_2) & \cosh(\gamma_0 l_2) \end{bmatrix} \\ &\quad \cdot \begin{bmatrix} \cosh(\gamma_0\sqrt{\varepsilon_{eff}}\, l_s) & \frac{Z_c}{Z_0\sqrt{\varepsilon_{eff}}}\sinh(\gamma_0\sqrt{\varepsilon_{eff}}\, l_s) \\ \frac{Z_0\sqrt{\varepsilon_{eff}}}{Z_c}\sinh(\gamma_0\sqrt{\varepsilon_{eff}}\, l_s) & \cosh(\gamma_0\sqrt{\varepsilon_{eff}}\, l_s) \end{bmatrix} \\ &\quad \cdot \begin{bmatrix} \cosh(\gamma_0 l_2) & \frac{Z_c}{Z_0}\sinh(\gamma_0 l_2) \\ \frac{Z_0}{Z_c}\sinh(\gamma_0 l_2) & \cosh(\gamma_0 l_2) \end{bmatrix} \cdot \begin{bmatrix} \cosh(\gamma_1 l_1) & \sinh(\gamma_1 l_1) \\ \sinh(\gamma_1 l_1) & \cosh(\gamma_1 l_1) \end{bmatrix} \\ &= \begin{bmatrix} a_1 & b_1 \\ c_1 & d_1 \end{bmatrix} \end{aligned} \tag{9}$$

$$S_{21}^{sub} = \frac{2}{a_1 + b_1 + c_1 + d_1} \tag{10}$$

where S_{21}^{sub} is the transmission scatter parameter with the substrate loaded in the fixture and measured by VNA. The meanings of other variables are the same as those in Section 3.

Ignoring the change of effective permittivity [6], the cascaded ABCD matrix after being loaded with the thin film deposited on the substrate can be expressed as

$$\begin{aligned} A_2 &= \begin{bmatrix} \cosh(\gamma_1 l_1) & \sinh(\gamma_1 l_1) \\ \sinh(\gamma_1 l_1) & \cosh(\gamma_1 l_1) \end{bmatrix} \cdot \begin{bmatrix} \cosh(\gamma_0 l_2) & \frac{Z_c}{Z_0}\sinh(\gamma_0 l_2) \\ \frac{Z_0}{Z_c}\sinh(\gamma_0 l_2) & \cosh(\gamma_0 l_2) \end{bmatrix} \\ &\quad \cdot \begin{bmatrix} \cosh(\gamma_0\sqrt{\varepsilon_{eff}\mu_{eff}}l_s) & \frac{Z_c\sqrt{\mu_{eff}}}{Z_0\sqrt{\varepsilon_{eff}}}\sinh(\gamma_0\sqrt{\varepsilon_{eff}\mu_{eff}}l_s) \\ \frac{Z_0\sqrt{\varepsilon_{eff}}}{Z_c\sqrt{\mu_{eff}}}\sinh(\gamma_0\sqrt{\varepsilon_{eff}\mu_{eff}}l_s) & \cosh(\gamma_0\sqrt{\varepsilon_{eff}\mu_{eff}}l_s) \end{bmatrix} \\ &\quad \cdot \begin{bmatrix} \cosh(\gamma_0 l_2) & \frac{Z_c}{Z_0}\sinh(\gamma_0 l_2) \\ \frac{Z_0}{Z_c}\sinh(\gamma_0 l_2) & \cosh(\gamma_0 l_2) \end{bmatrix} \cdot \begin{bmatrix} \cosh(\gamma_1 l_1) & \sinh(\gamma_1 l_1) \\ \sinh(\gamma_1 l_1) & \cosh(\gamma_1 l_1) \end{bmatrix} \\ &= \begin{bmatrix} a_2 & b_2 \\ c_2 & d_2 \end{bmatrix} \end{aligned} \tag{11}$$

$$S_{21}^{film} = \frac{2}{a_2 + b_2 + c_2 + d_2} \tag{12}$$

where S_{21}^{film} is the transmission scatter parameter with the film loaded in the fixture and measured by VNA. Solving Equations (9) $\sim$ (12), the effective permeability can be determined. Then, the permeability of thin film can be obtained by Equation (8). And the perturbation of the thin film (ΔS_{21}) can be expressed as

$$\Delta S_{21} = \frac{S_{21}^{film}}{S_{21}^{sub}} \tag{13}$$

4. RESULTS

To validate and compare the two methods, the complex permeability of FeNi/CoFe multilayer thin film samples is measured from 100 MHz to 18 GHz by using the two constructed fixtures (shown in Figure 1 and Figure 3), respectively. The lengths of the microstrip is 30 mm for SMM while it is 50 mm for MTM. The substrate of the thin films has the size of 7 mm $\times$ 7 mm $\times$ 0.53 mm. And the thickness of the thin films is 90 nm. Agilent Technologies VNA N5230A is used to detect the perturbation by loading the samples in the fixture.

The complex permeability of thin film is measured by the two methods, and the theoretical result is also obtained from Landau-Lifshitz-Gilbert equation [9] (The saturation magnetization M_s and anisotropy constant K_u are measured as 1.41×10^6 A/m, and 1500 J/m^3, respectively. The gyromagnetic factor γ is approximately 176 GHz/T [9], and the damping constant α is 0.015 corresponding to our thin film). As shown in Figure 5, the two experimental results

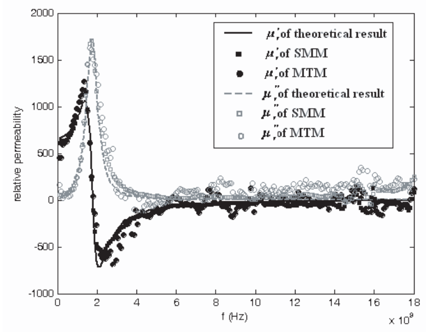

Figure 5. The complex permeability of the thin film.

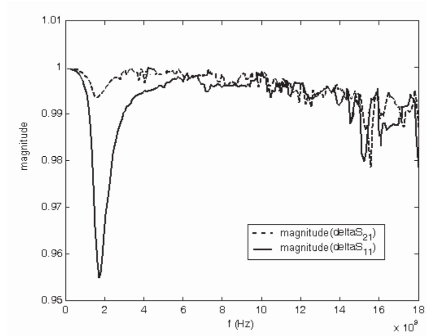

Figure 6. The magnitude perturbations after thin film loaded in the fixtures.

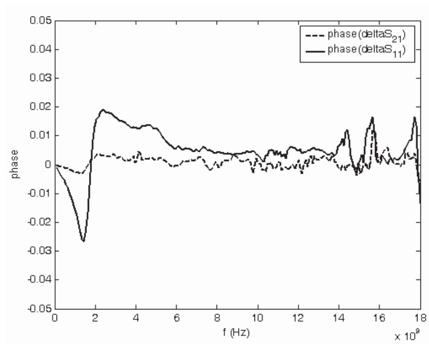

Figure 7. The phase perturbations after thin film loaded in the fixtures.

agree with the theoretical one closely up to 6 GHz. And when the operation frequency get higher, the result measured by SMM is closer to the theoretical result than the one measured by MTM.

The perturbations after the thin film loaded in these two fixtures are calculated and compared for analysis purpose. As shown in Figure 6, the magnitudes of both ΔS_{11} and ΔS_{21} dropped remarkably at about 1.7 GHz, which is led by the magnetic resonance of the thin film. And compared with ΔS_{21}, the magnitude of ΔS_{11} dropped more obviously, which means that the magnitude perturbation of SMM is stronger than that of MTM. As shown in Figure 7, the phase of both ΔS_{11} and ΔS_{21} changed remarkably from 100 MHz to 6 GHz due to the large real part of permeability. And compared with ΔS_{21}, the phase change of ΔS_{11} is more obvious; in other words, the phase perturbation of SMM is stronger than that of MTM, too. Because of the stronger perturbation, the SMM can reach a higher measurement sensitivity.

Further more, the comparison between SMM and MTM is based on the same size (w and h) of the microstrip. For both of these two methods, decreasing the distance between upper strip and ground can increase the perturbation and then improve the measurement sensitivity and accuracy.

5. CONCLUSION

In this paper, the complex permeability of ferromagnetic is measured by using shorted microstrip method and microstrip transmission method, respectively. The measurement fixtures are fabricated, and the cascade ABCD matrix networks are analyzed. From the experimental results one can see that the results obtained by the two methods agree with the theoretical results closely. And compared with the microstrip transmission method, the shorted microstrip method achieved higher measurement sensitivity and accuracy.

ACKNOWLEDGMENT

The authors wish to thank Weibo Wu (School of Microelectronics and Solid-state Electronics, University of Electronic Science and Technology of China) for providing the samples under test.

APPENDIX A.

$$q_1 = \frac{h_1}{2h} \cdot \left[1 + \frac{\pi}{4} - \frac{h}{w_{eff}} \cdot \ln\left(2w_{eff} \cdot \frac{\sin\left(\frac{\pi h_1}{2h}\right)}{h_1} + \cos\left(\frac{\pi h_1}{2h}\right) \right) \right] \quad \text{(A1)}$$

$$q_2 = \frac{h_1 + h_2}{2h} \cdot \left\{ 1 + \frac{\pi}{4} - \frac{h}{w_{eff}} \cdot \ln\left[2w_{eff} \cdot \frac{\sin\left(\pi \frac{h_1+h_2}{2h}\right)}{h_1 + h_2} \right.\right. \quad \text{(A2)}$$

$$\left.\left. + \cos\left(\pi \frac{h_1 + h_2}{2h}\right) \right] \right\} - q_1 \quad \text{(A3)}$$

$$q_3 = 1 - \frac{h}{2w_{eff}} \cdot \ln\left(\pi \frac{w_{eff}}{h} - 1\right) - q_2 - q_1 \quad \text{(A4)}$$

$$w_{eff} = w + \frac{2h}{\pi} \cdot \ln\left[17.08 \left(\frac{w}{2h} + 0.92 \right) \right] \quad \text{(A5)}$$

where w is the width of the upper strip; w_{eff} is the effective width of the upper strip; h is the distance between the upper strip and the ground; h_1 and h_2 are the thickness of thin film and substrate, respectively.

REFERENCES

1. Staostenko, S. N., K. N. Rozanov, and A. V. Osipov, "A broadband method to measure magnetic spectra of thin films," *J. Appl. Phys.*, Vol. 103, 07E914, 2008.
2. Adenot, A.-L., O. Acher, D. Pain, F. Duverger, M.-J. Malliavin, D. Damiani, and T. Taffary, "Broadband permeability measurement of ferromagnetic thin films or microwires by a coaxial line perturbation method," *J. Appl. Phys.*, Vol. 87, No. 9, 5965–5967, 2000.
3. Wu, Y., Z. Tang, Y. Xu, and B. Zhang, "An improved measurement configuration for determining the permeability of ferromagnetic thin film materials," *Journal of Electromagnetic Waves and Applications*, Vol. 22, No. 2–3, 343–352, 2008.
4. Kumar, A. V. P., V. Hamsakutty, J. Yohannan, and K. T. Mathew, "Microstripline FED cylindrical dielectric resonator antenna with a coplanar parasitic IC strip," *Progress In Electromagnetics Research*, PIER 60, 143–152, 2006.
5. Saed, M. A., "Reconfigurable broadband microstrip antenna FED by a coplanar waveguide," *Progress In Electromagnetics Research*, PIER 55, 227–239, 2005.
6. Liu, Y., L. Chen, C. Y. Tan, H. J. Liu, and C. K. Ong, "Broadband complex permeability characterization of magnetic thin films using shorted microstrip transmission-line perturbation," *Review of Scientific Instruments*, Vol. 76, 063911.1–063911.8, 2005.
7. Svačina, J., "A simple quasi-static determination of basic parameters of multilayer microstrip and coplanar waveguide," *IEEE Microwave and Guided Wave Letters*, Vol. 2, No. 10, October 1992.
8. Pucel, R. A. and D. J. Massé, "Microstrip propagation on magnetic substrates-Part I: Design theory," *IEEE Trans. MTT*, Vol. 20, No. 5, 304–308, May 1972.
9. Huijbregtse, J., F. Roozeboom, J. Sietsma, J. Donkers, T. Kuiper, and E. van de Riet, "High-frequency permeability of soft-magnetic Fe-Hf-O films with high resistivity," *J. Appl. Phys.*, Vol. 83, No. 3, 1569–1574, February 1998.